2000年度 大韓電子工學會 夏季綜合學術大會 論文集 第 23 卷 第1號 2000/6

# Independent Component Analysis for the Blind Separation Of Spatially Independent Components From $H_2{}^{15}O$ Dynamic Myocardial Positron Emission Tomography

이 재 성, 안 지 영, 이 동 수, 박 광 석
서울대학교 의과대학 의공학교실, 핵의학교실
전화 : (02) 760-3135 / 팩스 : (02) 745-7870

Jae Sung Lee, Ji Young Ahn, Dong Soo Lee, Kwang Suk Park
Deparment of Biomedical Engineering and Nuclear Medicine, Seoul National University College of Medicine
E-mail : kspark@snuvh.snu.ac.kr

## Abstract

We applied the ICA method to separate the ventricle and tissue components and to extract left ventricular input function from the $H_2{}^{15}O$ myocardial PET under the assumption that the elementary activities of ventricular pools and myocardium were spatially independent, and that the mixture of them composed dynamic PET frames. ICA-generated left ventricular input functions were compared with the ROI-generated ones, and also with the invasively derived arterial blood samples. Moreover, the rMBF calculated with the ICA-generated input functions and single compartment model was correlated with the results obtained with the radiolabeled microspheres.

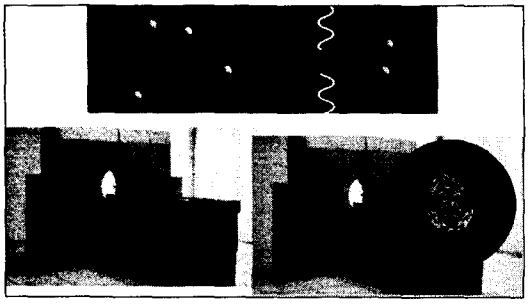

Fig. 1. Positron Emission Tomography (PET)

## I. Introduction

Based on the differential equation for the kinetics of radiopharmaceutical, regional myocardial blood flow (rMBF) can be estimated using the time activity curve (TAC) of the blood pool and myocardial tissue measured by positron emission tomography (PET). In the quantification of rMBF using $H_2{}^{15}O$ dynamic PET, the input TAC could be obtained by sampling the blood from the artery or by drawing the region of interest (ROI) on the left ventricular (LV) area in the PET image. Arterial blood sampling is too uncomfortable method for both the patients and operator since it should be performed several times during the PET scanning in rapid manner. In contrast, the non-invasiveness in the method of drawing the ROI could reduce the patients and operator' s burden.

It is, however, hard to identify the anatomical structure of the LV on a PET image to draw the ROI. The reason is because $H_2{}^{15}O$ with bolus injection is rapidly and evenly distributed over the whole cardiac regions, such as the left and right ventricle (RV) and myocardial tissues.

Biomedical application of the blind source separation by Independent Component Analysis (ICA) has received considerable attention because of its plausibility to biomedical signals. In this study we applied this fairly novel approach to the problem

of noninvasive extraction of LV input function from the $H_2{}^{15}O$ dynamic myocardial PET image.

## II. Independent Component Analysis

Let' s assume an N-dimensional zero-mean random variable $s(t)=[s_1(t), \cdots, s_N(t)]^T$, such that the components si(t) are mutually independent. In real environment we can observe mixed signal x(t) at each time point t, such that x(t)=As(t). The goal of blind source separation using ICA is to find a linear transformation W of the mixed signal x(t) in order to make the outputs, u(t)=Wx(t), as independent as possible.

*Information maximization approach* provides a general learning rule for ICA. The learning rule can be derived by maximizing the output entropy H(y). The joint entropy at the outputs is

$$H(y)=H(y_1,\cdots,y_N)=H(y_1)+\cdots+H(y_N)-I(y_1,\cdots,y_N),$$

where $H(y_i)$ are the marginal entropies of the outputs and $I(y_1,\cdots,y_N)$ is their mutual information. Extended infomax learning algorithm to maximize the joint entropy provides a simple learning rule for sources with a variety of distributions.

Extended infomax learning rule can be summarized as following equations,

$$\triangle W \propto [\ I-K\tanh(u)u^T- uu^T\ ]W$$

where K is an N-dimensional diagonal matrix of which element ki must be

$$k_i = \mathrm{sign}(E\{\mathrm{sech}^2(u_i)\}E\{u_i^2\}-E\{[\tanh(u_i)]u_i\}).$$

## III. Methods

555~740 Mbq $H_2{}^{15}O$ was injected to 6 dogs at rest and stress and dynamic PET scans were performed. On the transverse slices of static images containing the biggest heart, original images were masked to reduce the extracardiac noise and include only cardiac components. The 32×32×4 (pixel×pixel×plane) selected dynamic images with 24 frames were summed to four input vectors for ICA. All the data points were passed 1000 times through the learning rule using a block size of 10 for batch learning. The learning rate was fixed at 0.0005. Parametric maps of the covariance between each

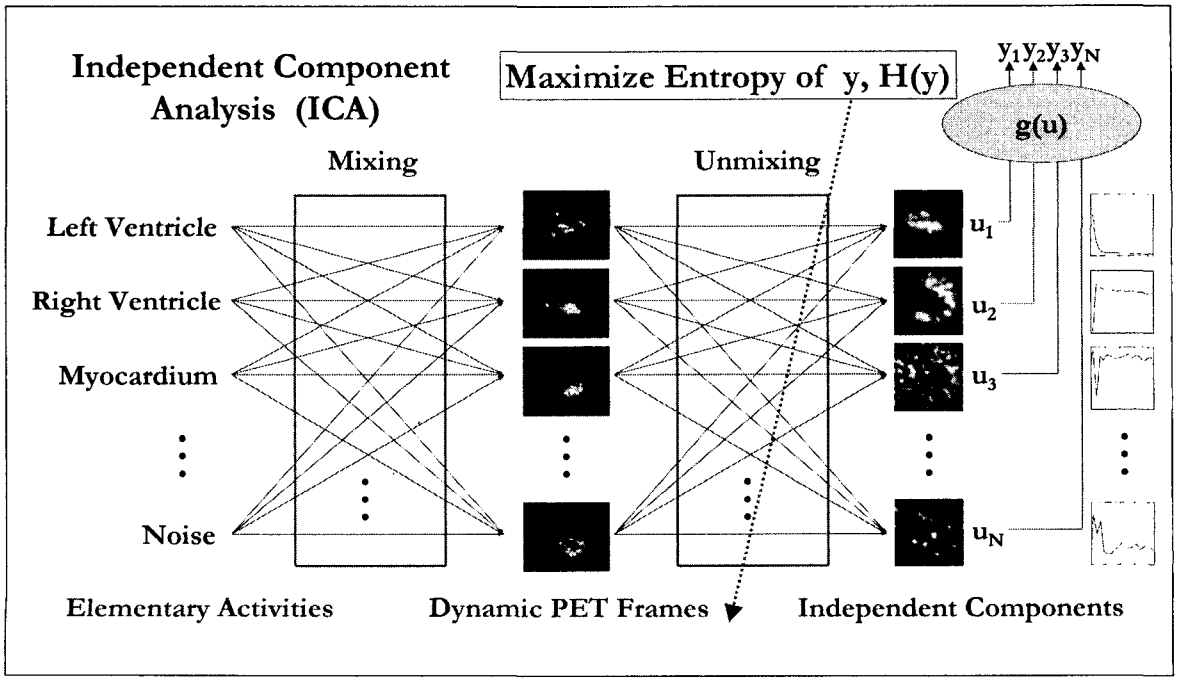


Fig. 2. Schematic diagram of ICA

voxel and resulting independent component were composed.

Independent components for LV and RV were rescaled by the maximum values in the ventricular pools that were extracted from the parametric maps of the covariance.

We computed rMBFs using the input function by the ICA and compared them with those by the ROI method. Tissue and blood pool TACs were obtained from the manually drawn ROI on the image of myocardium that was made by simple subtraction of the initial 30 seconds' image from the two minute s' one.

rMBF was estimated using single compartment model. Moreover, the rMBF calculated with the ICA-generated input functions and single compartment model was correlated with the results obtained with the radiolabeled microspheres (n=5 dogs).

## IV. Results

In all the cases, LV input functions were extracted successfully by the ICA method. The log-likelihood increased rapidly and reached plateau between 15 and 20 repetition of training. The results were consistent in all the canine studies. Even though we realized the ICA algorithm and reading process of PET image by the low speed computer language, Matlab (Mathworks, Natick, Mass., USA), computation time for whole process was less than 15 seconds on the workstation with 333 MHz CPU and 128 MB memory (DEC AlphaStation 600, Digital Equipment Corp., Maynard, Mass., USA).

Figure 3 shows the resulting independent component images. ICA-generated input functions showed good correlation with the ROI-generated ones (relative error=4.9±1.8%), and showed similar shape with the arterial samples except for the time lags. LV activities by the ICA and blood sampling are compared in Figure 4.

rMBF with ICA was in agreement with the previously reported values and showed good correlation with the result by microsphere ($r=0.95$, $p<0.0001$) (Fig. 5 and 6).

## V. Conclusion

Using the blind source seperation by ICA, we could non-invasively extract the input function for the compartment modeling of myocardial perfusion from the $H_2{}^{15}O$ PET images. The rMBF using the LV activity by the ICA as the input function was correlated well with that by the ROI method. Since all the process was automatically achieved with very short computation time, it will be clinically useful for the quantification of the rMBF using $H_2{}^{15}O$ dynamic PET.

## VI. References

[1] S. R. Bergmann, K. A. A. Fox, A. L. Rand, K. D. McElvany, M. J. Welch, J. Markhan, B. E. Sobel, Quantification of regional myocardial blood flow in vivo with $H_2{}^{15}O$ , Circulation, Vol. 70, pp. 724-733, 1984.

[2] J. Y. Ahn, J. S. Lee, D. S. Lee, J. M. Jeong, J-K. Chung, M. C. Lee, Multi-plane factor analysis for extracting input functions and tissue curves from O-15 water dynamic myocardial PET , J Nucl Med, Vol. 40(5), p. 77, 1999.

[3] A. S. Houston, The effect of apex-finding errors on factor images obtained from factor analysis and oblique transformation , Phys Med Biol, Vol. 29, pp. 1109-1116, 1984.

[4] A. S. Houston, W. F. D. Sampson, A quantitative comparison of some FADS methods in renal dynamic studies using simulated and phantom data , Phys Med Biol, Vol. 42, PP. 199-217, 1997.

[5] M. J. McKeown, S. Makeig, G. G. Brown, T-P. Jung, S. S. Kindermann, A. J. Bell, T. J. Sejnowski, Analysis of fMRI data by blind separation into independent components , Human Brain Mapping, Vol. 6, pp. 1-31, 1998.

[6] S. Makeig, M. Westerfield, T-P. Jung, J. Covington, J. Townsend, T. J. Sejnowski, E. Courchesne, Independent components of the late positive .event-related potential in a visual spatial attention task Journal of Neuroscience, Vol. 19, pp. 2665-2680, 1999.

[7] T-W. Lee, Independent component analysis: theory and applications, Boston: Kluwer Academic Publishers., 1998.

[8] S. Haykin, Neural network: a comprehensive

foundation, UK, London: Prentice-Hall, Inc., pp. 484-544, 1999.

[9] A. J. Bell, T. J. Sejnowski, An information-maximisation approach to blind separation and blind deconvolution , Neural Computation, Vol. 7, pp. 1004-1034, 1995.

[10] T-W. Lee, M. Girolami, T.J. Sejnowski, Independent component analysis using an extended infomax algorithm for mixed sub-gaussian and super-gaussian sources , Neural Computation, Vol. 11, pp. 417-441, 1999.

[11] H-M. Wu, C. K. Hoh, D. B. Buxton, W. G. Kuhle, H. R. Schelbert, Y. Choi, R. A. Hawkins, M. E. Phelps, S-C. Huang, Quantification of myocardial blood flow using dynamic nitrogen-13-ammonia PET studies and factor analysis of dynamic structures , J Nucl Med, Vol. 36, pp. 2087-2093, 1995.

[12] P. Herrero, J. Markham, D. W. Myears, C. J. Weiheimer, S. R. Bergmann, Measurement of myocardial blood flow with positron emission tomography: correction for count spillover and partial volume effects , Math Comput Model, Vol. 11, pp. 807-812, 1988.

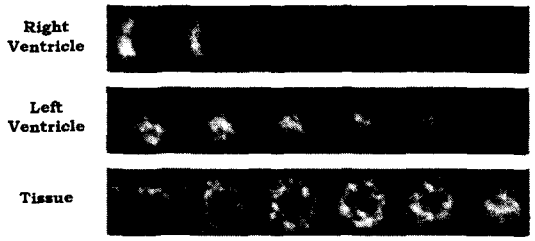


Fig. 3. Extracted independent components

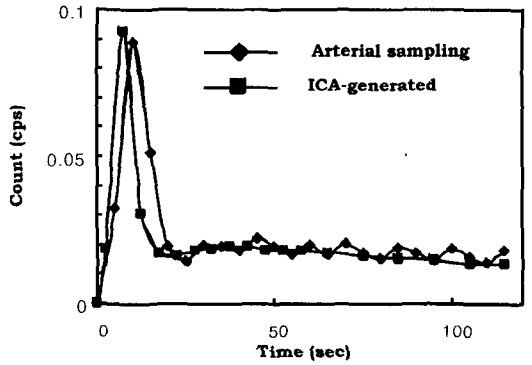


Fig. 4. Left ventricular blood pool activity obtained by ICA and arterial blood sampling

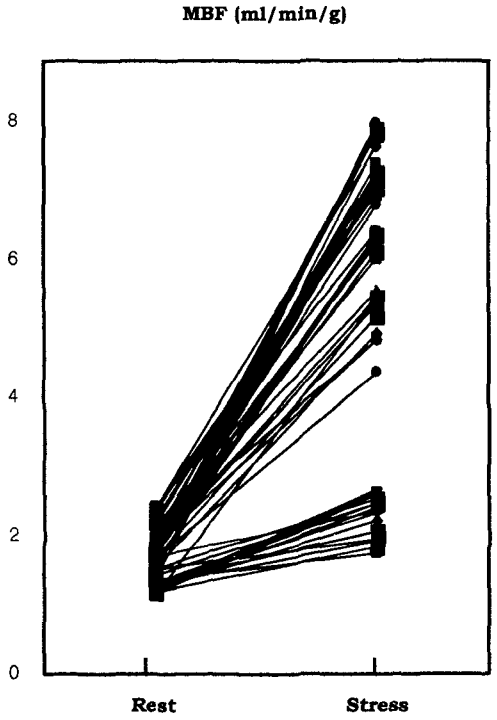


Fig. 5. Regional myocardial blood flow obtained using ICA under rest and after pharmachological stress

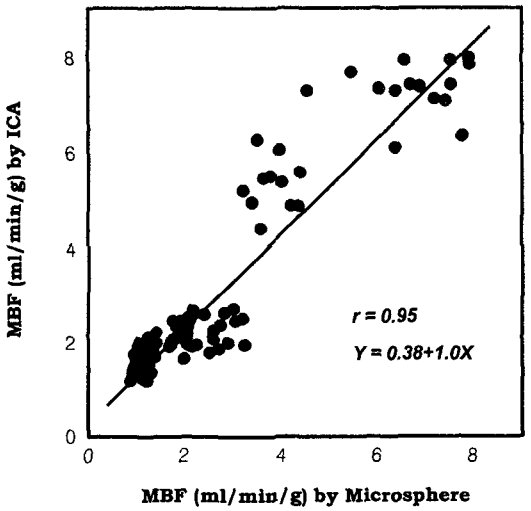


Fig. 6. Correlation between blood flows obtained using ICA and microsphere technique